HHS Public Access

Author manuscript

Glia. Author manuscript; available in PMC 2018 August 01.

Published in final edited form as:

Glia. 2017 August ; 65(8): 1302–1316. doi:10.1002/glia.23163.

Reduced gliotransmitter release from astrocytes mediates tau-induced synaptic dysfunction in cultured hippocampal neurons

Roberto Piacentini[1,#], **Domenica Donatella Li Puma**[1,#], **Marco Mainardi**[1], **Giacomo Lazzarino**[2], **Barbara Tavazzi**[2], **Ottavio Arancio**[3], and **Claudio Grassi**[1,*]

[1]Institute of Human Physiology, Medical School, Università Cattolica, Largo F. Vito 1, 00168, Rome, Italy

[2]Institute of Biochemistry and Clinical Biochemistry, Medical School, Università Cattolica, Largo F. Vito 1, 00168, Rome, Italy

[3]Department of Pathology and Cell Biology and Taub Institute for Research on Alzheimer's Disease and the Aging Brain, Columbia University, New York, 630 W 168th St., NY 10032 USA

Abstract

Tau is a microtubule-associated protein exerting several physiological functions in neurons. In Alzheimer's disease (AD) misfolded tau accumulates intraneuronally and leads to axonal degeneration. However, tau has also been found in the extracellular medium. Recent studies indicated that extracellular tau uploaded from neurons causes synaptic dysfunction and contributes to tau pathology propagation. Here we report novel evidence that extracellular tau oligomers are abundantly and rapidly accumulated in astrocytes where they disrupt intracellular Ca^{2+} signaling and Ca^{2+}-dependent release of gliotransmitters, especially ATP. Consequently, synaptic vesicle release, the expression of pre- and post-synaptic proteins, and mEPSC frequency and amplitude were reduced in neighboring neurons. Notably, we found that tau uploading from astrocytes required the amyloid precursor protein, APP. Collectively, our findings suggests that astrocytes play a critical role in the synaptotoxic effects of tau via reduced gliotransmitter availability, and that astrocytes are major determinants of tau pathology in AD.

Graphical abstract

[*]Corresponding Author: Claudio Grassi, Institute of Human Physiology, Università Cattolica, Largo Francesco Vito 1, 00168 Rome, Italy. claudio.grassi@unicatt.it. Phone: +39-06-3015-4966; Fax: +39-06-3015-4665.

[#]These authors contributed equally to this work

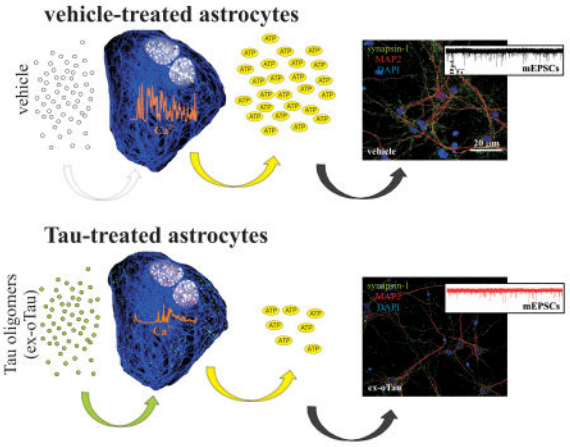

Keywords

Tauopathy; Tripartite synapse; Synaptic transmission; Synaptic proteins; APP

Introduction

The amyloid hypothesis has dominated the field of Alzheimer's disease (AD) pathogenesis in the last 30 years. However, increasing evidence demonstrates the pivotal role of tau protein in this pathology (Guerrero-Muñoz et al., 2015). Tau is a microtubule-associated protein primarily localized in the axons of neurons and its main physiological role is to stabilize microtubules. However, many other functions have been identified for this protein that include axonal transport, signal transduction, and neuronal polarization (Medina and Avila, 2014). Six tau isoforms are derived from alternative splicing of the microtubule-associated protein tau (MAPT) gene transcript in the adult brain, with the 4R/2N isoform being the longest one (Fà et al., 2016; Kampers et al., 1999). Tau protein is highly subjected to phosphorylation and in several pathologies, including AD, hyperphosphorylated and misfolded tau accumulates intraneuronally and leads to axonal degeneration, thus contributing to neuronal loss.

Although tau is an intracellular protein, full-length tau have also been found in the extracellular medium, mainly due to activity-dependent secretion from neurons and/or release from dead cells (Fà et al., 2016; Medina and Avila, 2014; Pooler et al., 2013; Yamada et al., 2014). Recent studies suggested that soluble extracellular tau aggregates impinge on the synaptic function (Fà et al., 2016; Guerrero-Muñoz et al., 2015; Lasagna-Reeves et al., 2011). We recently demonstrated that extracellular application of oligomeric tau (ex-oTau) inhibited synaptic plasticity at the CA3-CA1 synapses and impaired limbic system-dependent memory formation in mice (Fà et al., 2016). We also found that the synaptotoxic tau oligomers crossed plasma membranes of cultured hippocampal neurons and accumulated intracellularly whereas tau monomers, that did not exert any adverse effect on brain functions, are less prone to enter neurons (Fà et al., 2016; Wu et al., 2013;), though they enter SH-SY5Y neuroblastoma cells (Michel et al., 2013) where they may exert a toxic

action mediated by M1 and M3 muscarinic receptors activation (Díaz-Hernández et al., 2010).

In tauopathies, tau accumulation has also been found in cells others than neurons, i.e., astrocytes and microglia (Asai et al., 2015; Bolós et al., 2016; Forman et al., 2005; Kahlson and Colodner, 2016; Lasagna-Reeves et al., 2014; Maphis et al., 2015; Togo and Dickson, 2002). The role of microglia in tau pathology has been extensively investigated (Asai et al., 2015; Bolós et al., 2016; Luo et al., 2015; Maphis et al., 2015), whereas that of astrocytes remains unclear yet. In particular, so far no studies have addressed the role of astrocytes in tau-induced synaptic dysfunction. Astrocytes have several functions in the brain: besides providing structural and metabolic support to neurons, they directly modulate a number of neuronal functions (Giaume and Oliet, 2016). Specifically, they modulate synaptic transmission (Araque et al., 1998; Fields and Burnstock 2006; Jourdain et al., 2007; Perea and Araque 2010; Zorec et al., 2016a) and orchestrate synaptic plasticity (De Pittà et al., 2016). Astrocytes are indeed partner in the “tripartite synapse”: they exchange information with the synaptic neuronal elements, respond to synaptic activity and regulate synaptic transmission through the Ca^{2+}-dependent release of gliotransmitters such as ATP, glutamate and D-serine (Fields and Burnstock 2006; Zorec et al., 2016a). Therefore astrocytes are also actively involved in memory formation, and they may play a key role in neurodegenerative diseases (Gao et al., 2016; Verkhratsky at al., 2016; Zorec et al., 2016b).

Here, we tested the hypothesis that accumulation of tau oligomers in astrocytes contributed to tau-induced synaptic dysfunction by impinging on gliotransmitter release.

Materials and Methods

Primary cultures of hippocampal neurons and astrocytes

Co-cultures of hippocampal neurons and astrocytes were obtained from wild type (WT) E18 C57/bl6 mice as previously described (Maiti et al., 2011) with minor modifications. Primary cultures of cortical and/or hippocampal astrocytes were obtained from E18 C57/bl6 mice, CByJ.B6-Tg(CAG-EGFP)1Osb/J (eGFP expressing mice) and B6.129S7-Apptm1Dbo/J (APP KO) mice as previously described (Podda et al., 2012). Briefly, after removing brain, dissected cortices were incubated for 10 min at 37 °C in phosphate buffered saline (PBS) containing trypsin-ethylenediaminetetraacetic acid (0.025%/0.01% w/v; Biochrom AG, Berlin, Germany) and the tissue was mechanically dissociated at room temperature [(RT), 23-25 °C] with a fire-polished Pasteur pipette. The cell suspension was harvested and centrifuged at 235 × g for 8 min. Then, for co-cultures of neurons and astrocytes, the pellet was suspended in 88.8% Minimum Essential Medium (MEM, Biochrom), 5% fetal bovine serum (FBS), 5% horse serum, 1% glutamine (2 mM), 1% penicillin-streptomycin-neomycin antibiotic mixture (PSN, Thermo Fisher Scientific, Waltham, MA, USA), and glucose (25 mM). Cells were plated at a density of 10^5 cells on 20-mm coverslips (for immunocytochemical, patch-clamp and FM1-43 studies) and 10^6 cells/well on 35-mm six-well plates (for Western blot studies), precoated with poly-L-lysine (0.1 mg/ml; Sigma, St. Louis, MO, USA). Twenty-four hours later, the culture medium was replaced with a mixture of 96.5% Neurobasal medium (Thermo), 2% B-27 (Thermo), 0.5% glutamine (2 mM), and 1% PSN. After 72 h, this medium was replaced with a glutamine-free version of the same

medium, and the cells were grown for 10 more days before carrying-out experiments. For primary cultures of hippocampal and/or cortical astrocytes, the suspension of single cells (obtained as before) was suspended in a medium consisting of MEM with 3.7 g/L $NaHCO_3$ and 1.0 g/L D-glucose, 5% FBS, 1% PSN and then placed in cell culture flasks. The culture the medium was changed within 24 hours of seeding and twice weekly thereafter. After cell expansion, astrocytes were plated at high density on 20-mm coverslips (for Ca^{2+} imaging and immunocytochemical studies) or 35-mm six-well plates for HPLC measures. For co-cultures of APP KO astrocytes and WT hippocampal neurons, primary cultures of APP KO astrocytes were prepared as described above and plated onto 12-mm coverslips. When the astrocytes had formed a monolayer, hippocampal neurons were plated on at low density (15,000 cells/well, in order avoid contamination of APP-KO astrocytes with WT astrocytes) in neuronal culture medium (see above).

Recombinant tau preparation and oligomerization

Recombinant tau protein was prepared from the 4R/2N construct containing C-terminal 6× His-tag expressed in *Escherichia coli* (Rosetta), as previously described in Fà et al., 2016. Oligomerization was achieved through incubation with 1 mM H_2O_2 at room temperature for 20 hours. Upon oligomerization excess H_2O_2 was removed from the sample by buffer exchange. Tau protein concentration was determined from the absorption at 280 nm with an extinction coefficient of 7450 cm^{-1} M^{-1}.

Human AD Tau preparation

AD Tau was isolated as previously described (Fà et al., 2016) from prefrontal/frontal cortex of AD patients. Human tissue was provided by the New York Brain Bank–The Taub Institute, Columbia University. Tissue was homogenized in acidic buffer containing 1% perchloric acid, purified by anion exchange chromatography and oligomerized as described above.

Assessment of tau uploading into cultured neurons and astrocytes

Oligomeric tau preparations were labelled with the IRIS 5-NHS active ester dye (IRIS 5; λ_{ex}: 633 nm; λ_{em}: 650-700 nm; Cyanine Technology, Turin, Italy) as previously described (Fà et al., 2016). Briefly, tau solutions (2 μM in PBS) were mixed with 6 mM IRIS 5 in dimethyl sulfoxide for 4 hours in the dark under mild shaking conditions. After this time, labeled tau was purified with Vivacon 500 ultrafiltration spin columns (Sartorius Stedim Biotech GmbH, Goettingen, Germany) and then resuspended in PBS and used at final concentration of 100 nM. Immunocytochemistry and confocal microscopy were performed in cells treated with IRIS 5-labelled oligomeric tau for either 1 or 7 hours. All experiments were repeated at least 3 times. To quantify the amount of cellular internalization of tau, the parameter “internalization index” was introduced by multiplying the percentage of astrocytes or neurons internalizing fluorescent proteins in each analyzed microscopic field by the mean number of fluorescent spots inside cells.

Confocal Ca^{2+} imaging

Confocal Ca^{2+} imaging was performed as previously described (Iacopino et al., 2014; Santoro et al., 2014) with minor modifications. Briefly, cultured hippocampal astrocytes (either WT or APP KO) were incubated for 30 min at 37 °C with the Ca^{2+} sensitive fluorescent dye Fluo-4 AM (2.5 μM, Thermo) in Tyrode's solution containing (in mM): 150 NaCl, 4KCl, $1MgCl_2$, 10 glucose, 10 HEPES and 2 $CaCl_2$ (pH adjusted to 7.4 with NaOH). The dye-loaded cells were washed and maintained on coverslips for 20 min at RT in fresh Tyrode's solution to allow complete dye de-esterification. Coverslips were then transferred to a perfusion chamber placed on the stage of an inverted confocal microscope (TCS-SP2; Leica). Fluo-4-loaded cells were excited with the 488-nm line of an Ar/ArKr laser, and the emission signal was collected by a photomultiplier within a spectral window ranging from 500 to 535 nm. The amplitude of Ca^{2+} signals was estimated as $\Delta F/F = (F_t - F_{pre})/(F_{pre} - F_{bgnd})$, where F_t is the mean of fluorescence intensities measured at a given time (t) in a region of interest (ROI) traced around each cell body; F_{pre} is the basal fluorescence intensity in this ROI; and F_{bgnd} is background fluorescence intensity measured in an area of the imaged field lacking dye-filled structures. Intracellular Ca^{2+} transients were obtained following ATP exposure (100 μM for 10 s). Intracellular Ca^{2+} waves triggered by ATP stimulation were studied throughout 30-min recordings.

High Performance Liquid Chromatography (HPLC) measurements

For HPLC measurements astrocytes were cultured in 30-mm wells and treated for 1 hour with tau or vehicle in Tyrode's solution. At the end of treatment tau- or vehicle-containing Tyrode's solution was withdrawn from each well and samples were deproteinized as described in details elsewhere (Tavazzi et al., 2005). Briefly, samples were transferred to an Eppendorf tube equipped with a filtering membrane of 3KDa cut-off (Nanosep® Centrifugal Devices, Pall Gelman Laboratory, Ann Arbor, MI, USA) and centrifuged at 10,500 × *g* for 30 min at 4 °C. The protein-free ultrafiltrate fluids were directly injected onto the HPLC column and analyzed to determine concentrations of ATP, ADP, glutamate (Glu), glutamine (Gln) and serines (Ser, both L- and D-). The two nucleotides were separated and quantified according to an ion-pairing HPLC method previously set up (Tavazzi et al., 2005), whilst the amino acids were analyzed as ortophtalaldehyde (OPA) derivatives using a different method with pre-column derivatization (Amorini et al., 2012; Amorini et al., 2016). For both analyses, the HPLC apparatus consisted of a SpectraSystem P4000 pump and a highly sensitive UV6000LP diode array detector (ThermoElectron Italia), equipped with a 5-cm light-path flow cell, set up between 200 and 400 nm wavelength for acquisition of chromatographic runs. Data were acquired and analyzed by ChromQuest® software package provided by the HPLC manufacturer. Separation of the various compounds was carried out using a Hypersil 250 × 4.6 mm, 5 μm particle-size column, which was provided with its own guard column (ThermoElectron Italia). Species identification and quantification in deproteinized samples of extracellular medium was determined by matching retention times, peak areas and absorption spectra of those of freshly prepared ultrapure standards. If needed, co-chromatograms were performed by adding proper standards with known concentration to the medium samples. The concentrations of ATP and ADP were determined at 260 nm wavelength and those of OPA-derivatized amino acids were calculated at 338 nm wavelength.

Whole-cell patch-clamp recordings

Electrophysiological recordings were carried out as described in Ripoli et al. (2013 and 2014) with some modifications. Briefly, neuronal cultures were maintained at RT in an external Tyrode's solution containing 4 mM $CaCl_2$ instead of 2 mM. Patch pipettes, fabricated from borosilicate glass capillaries with the aid of a micropipette puller (P-97; Sutter Instruments) had resistances of 4–6 MΩ when filled with an internal solution that contained the following (in mM): 146 K-gluconate, 18 HEPES, 1 EGTA, 4.6 $MgCl_2$, 4 MgATP 4, 0.3 Na_2GTP, 15 phosphocreatine (all chemicals were purchased from Sigma). Access resistance and membrane capacity were monitored before and at the end of the experiments to evaluate recording stability and cell health. Recordings were considered to be stable when the series and input resistances and resting membrane potential varied less than 20% of the initial value. Recordings were obtained with a Multiclamp 700B amplifier, connected to a Digidata 1440 series digital interface and Clampex 10.4 software (Molecular Devices, Sunnyvale, CA). After establishing a gigaseal, the cell membrane was ruptured to establish the whole-cell configuration, then at least 3 min were allowed for patch stabilization and cytosol dialysis. The membrane potential was voltage-clamped at -70 mV and miniature excitatory post-synaptic currents (mEPSCs) were recorded in 60-s epochs. All electrophysiological recordings were analyzed using the Clampfit 10.6 software (Molecular Devices). For mEPSC frequency analysis, a template was constructed using the “Event detection / create template” function, as previously described in Ripoli et al. (2013). Then, mEPSCs were detected using the “Event detection / template search” function; the “template match threshold” was set to 3.5 and the result inspected for false positives. For mEPSC amplitude analysis, all the waveforms detected during a single recording using template analysis were averaged and the corresponding amplitude calculated.

Immunocytochemistry

Immunocytochemistry was performed as previously described (Ripoli et al., 2013; Piacentini et al., 2015). Cells were treated with oligomeric tau (100 nM, either native or labelled with IRIS-5) for 1 hour and then fixed with 10% formalin solution neutral buffer (Sigma) for 10 min at RT. After being permeabilized (15 min incubation with 0.3% Triton X-100 [Sigma] in PBS), cells were incubated for 20 min with 0.3% BSA in PBS to block nonspecific binding sites. Hippocampal co-cultures of astrocytes and neurons cells were incubated overnight at 4 °C with different pairs of the following antibodies in the blocking solution: rabbit anti-microtubule associated protein 2 (MAP2, 1:500; Sigma) and mouse anti glial fibrillary acidic protein (GFAP, 1:500; Cell Signalling Technology Inc., Danvers, MA); or mouse anti-MAP2 (1:500; Immunological Sciences, Rome, Italy) and rabbit anti-synapsin-1 XP (1:300; Cell Signalling); or rabbit anti-MAP2 (1:500; Sigma) and mouse anti-synaptophysin (1:300; Immunological Sciences); or mouse anti-MAP2 and rabbit anti-GluR1 (1:300; Cell Signaling); or mouse anti-MAP2 and rabbit anti-PSD-95 (1:300; Cell Signaling). The next day, cells were incubated for 90 min at RT with a mixture of the following secondary antibodies: Alexa Fluor 546 donkey anti-rabbit (1:1,000; Thermo) and Alexa Fluor 488 donkey anti-mouse (1:1,000; Thermo). Finally, nuclei were counterstained with 4′,6-diamidino-2-phenylindole (DAPI, 0.5 μg/mL for 10 min; Thermo), and cells were coverslipped with ProLong Gold anti-fade reagent (Thermo).

To study dendritic spines, cells were incubated overnight with mouse anti-MAP-2 (1:500; Immunological Sciences) and the next day incubated with Alexa Fluor 488 anti-mouse for 90 min. After this treatment cells were treated with rhodamine-labelled phalloidine (Thermo) to stain F-actin, that is markedly expressed in dendritic spines.

For co-cultures of APP-KO astrocytes and WT astrocytes expressing eGFP, cells were incubated overnight at 4 °C with mouse anti glial fibrillary acidic protein (GFAP, 1:500, Cell Signalling). The next day, cells were incubated for 90 min at RT with the secondary antibodies Alexa Fluor 488 donkey anti-mouse (1:1,000; Thermo).

Confocal stacks made of images (1024×1024 pixels) were acquired at 60× magnification with a confocal laser scanning system (A1+, Nikon, Tokyo, Japan) and an oil-immersion objective (N.A. 1.4; physical pixel size: 210 nm). For some images, additional 2× magnification was applied. Fluorescent dyes were excited with diode lasers (405, 488, 546 and 633 nm). All experiments were repeated at least 3 times, and at least 10 randomly chosen microscopic fields were analyzed for each condition.

Hippocampal slice cultures and immunohistochemistry

Hippocampal organotypic slice (350 μm) cultures were prepared from postnatal day 4-7 Wistar rats through a McIllwain tissue chopper as described in Bosch et al., 2014. Cutting solution contained the following (in mM): 2.5 KCl, 25.6 $NaHCO_3$, 1.15 $NaHPO_4$, 11 D-Glucose, 238 Sucrose, 1 $CaCl_2$ and 5 $MgCl_2$. Slices were cultured at 35°C on interface membranes (Millipore) and fed with MEM media containing 20% horse serum (GIBCO), 27 mM D-glucose, 6 mM $NaHCO_3$, 1 mM $CaCl_2$, 1 mM $MgSO_4$, 30 mM HEPES, 0.01 % ascorbic acid and 1 μg/ml insulin. pH was adjusted to 7.3 and osmolality to 300-320 mOsm. Medium was changed every 48 h. After 10-day culture organotypic slice were treated with 100 nM of fluorescent IRIS-5 labelled oTau for 1 hour and then fixed overnight at 4°C with paraformaldehyde (4% in PBS). The following day slices were incubated with blocking buffer containing PBS with 3% normal goat serum (NGS, Sigma) and 2% Triton-X 100 for 2 hours at RT. The following day, slices were treated with one of the following primary antibodies diluted 1:200 in PBS containing 1% NGS and 0.5 %Triton-X100: rabbit anti-GFAP (Cell Signalling); rabbit anti-IBA1 (Biocare Medical, Pacheco, CA); and rabbit anti NeuN (1Cell Signalling) were for 48 h at 4°C. Then, slices were incubated with secondary antibody Alexa Fluor 488 donkey anti-rabbit (1:500; Thermo) for 2h at RT and nuclei were counterstained with (DAPI, 1:1000; Thermo). Finally, slices were coverslipped with ProLong Gold anti-fade reagent (Thermo). Confocal stacks made of images (1024×1024 pixels) were acquired at 40× magnification with a confocal laser scanning system (A1+, Nikon) and an oil-immersion objective (N.A. 1.4; physical pixel size: 210 nm). Additional 3× magnification was applied. Fluorescent dyes were excited with diode lasers (405, 488 and 633 nm).

Western Blot

Western blot experiments were carried out as previously described (Ripoli et al., 2013; Piacentini et al., 2015). Wild-type hippocampal neurons cultured with either WT or APP KO astrocytes for 14 days *in vitro* (DIV) were treated with 100 nM oTau or vehicle for 1 hour

prior to be washed twice with PBS and scraped in cold RIPA buffer containing 1 mM phenylmethylsulfonyl fluoride, phosphatase and protease inhibitor mixtures (Sigma), and 0,1% sodium dodecyl sulfate. After incubation for 15 min on ice, cellular suspensions were centrifuged (10,000 × g for 30 min at 4 °C) and the supernatants were collected and assayed to determine their protein concentration (Micro BCA protein assay, Thermo). Equivalent amounts of proteins (50 μg) were loaded onto either 10% tris-glycine polyacrylamide gels for electrophoretic separation and then electroblotted onto nitrocellulose membranes for Western blot analysis. Membranes were blocked with 5% nonfat dry milk in tris-buffered saline containing 0.1% Tween-20 for 1 hour at RT and incubated with primary antibodies (rabbit polyclonal anti synapsin-1 XP, Cell Signaling; mouse monoclonal anti synapthophysin, Immunological Science; rabbit polyclonal anti GluR1, Millipore; anti rabbit PSD-95, Cell Signaling; mouse monoclonal anti-α tubulin, Sigma; at a final concentration of 1 μg/mL). After incubation with appropriate secondary horseradish peroxidase-conjugated antibodies (1:2,000; Cell Signaling), visualization was performed with ECL plus (GE Healthcare, Amersham Place, Buckinghamshire) using either UVItec Cambridge Alliance. Molecular weights for immunoblot analysis were determined using BenchMark™ Pre-Stained Protein Ladder (Thermo). Densitometric analysis was carried out with Image J software. Experiments were repeated at least 3 times.

FM1-43 imaging

FM1-43 imaging was performed as described (Gaffield and Betz, 2006), with some modification. Briefly, culture medium of mouse hippocampal neurons cultured on 20-mm diameter glasses was replaced with Tyrode's solution and after 2 min cells were exposed for 1 min to 5 μM FM1-43 (Thermo) in Tyrode's solution. After this time, cells were exposed for 1 min to 5 μM FM1-43 in depolarizing Tyrode's solution (containing 50 mM KCl) in order to induce massive vesicle release and vesicle staining with FM1-43. After this step, cells returned to normal Tyrode's solution containing FM1-43 for 1 min and then in Tyrode's solution containing 200 μM Advasep™-7 (Sigma) for 2 min. FM1-43 fluorescence was excited by Argon laser at 488 nm and fluorescence recorded in a spectral window ranging from 520 to 650 nm. FM1-43 destaining was obtained by re-exposing FM1-43 labelled cells to 50 mM KCl for 1 min in normal Tyrode's solution.

Statistics

Statistical comparisons were performed with Systat 10.2 software. All data were expressed as mean ± standard error of the mean (SEM) and followed normal distribution, as assessed by the same software. In order to assess whether tau treatment significantly affected the measured parameters, the two-tailed Student's *t* test was used. One-way ANOVA with Student-Newman-Keuls's (SNK) *post-hoc* test was used for multiple-comparisons. For experiments that included fewer than 10 observations (e.g. densitometric analysis of western blotting data), or for non-normally distributed data, the Mann-Whitney (Wilcoxon) statistic was used. The level of significance was set at 0.05.

In all experiments the operators were blind to the study conditions.

Ethics Statement

All methods were carried out in accordance with the guidelines approved by the Ethics Committee of the Catholic University. All experimental and animal procedures were fully compliant with Italian (Ministry of Health guidelines, Legislative Decree No. 116/1992) and European Union (Directive No. 86/609/EEC) legislation on animal research. Efforts were made to limit the number of animals used and to minimize their suffering.

Results

Tau protein enters astrocytes more efficiently than neurons *in vitro*

We started investigating tau internalization in mixed cultures of hippocampal astrocytes and neurons obtained from C57/bl6 mice. To address this issue we labeled the N-terminus of tau with the fluorophore IRIS-5 ester dye and studied its intracellular localization by confocal microscopy. One hour after the extracellular application of IRIS-5-labelled oligomeric recombinant human tau (4R/2N; oTau, 100 nM), we found a more abundant and rapid accumulation of the protein in astrocytes than in neurons. In fact, at the end of the treatment, only a few fluorescent puncta corresponding to tau oligomers were found in neurons (identified by MAP2 immunoreactivity), compared to the high number of puncta observed in astrocytes (GFAP-positive cells; Fig. 1).

We quantified the intracellular accumulation of ex-oTau in the two cellular populations of our culture, i.e., MAP2-positive and GFAP-positive cells. We found that 96±3% of astrocytes (n=71 cells analyzed in 14 fields) and 85±6% of the neurons (n=41 cells in 14 microscopic fields) exhibited tau accumulation. Notably, the mean number of intracellular fluorescent spots was significantly higher in astrocytes (11.3±1.0) than in neurons (2.5±0.3). To provide an overall estimate of the protein uploading from these two cell populations we defined the “internalization index” (see methods) that was 12.6±1.9 for astrocytes and 2.5±0.5 for neurons ($P=5.14\times10^{-5}$ assessed by Student's *t* test; t=-4.9, dof=25; Fig. 1D). We also validated our findings in a more complex system. Specifically, the fluorescently-labelled oTau (IRIS-5, 100 nM) applied to the culture medium of organotypic brain slices for 1 hour was uploaded by astrocytes (GFAP-positive) and microglia (IBA1-positive), but very poorly by neurons (NeuN-positive cells; Supplementary Fig. 1).

Collectively, these data indicate that astrocytes exhibit much greater avidity for tau than neurons. Based on these results, short-lasting (i.e., 1-hour) ex-oTau treatments of hippocampal neuron and astrocyte co-cultures were used in subsequent experiments to determine the specific contribution of astrocytes to tau-induced synaptic dysfunction.

Tau treatment affects intracellular Ca^{2+} signals in cultured astrocytes

We then analyzed the functional alterations induced by ex-oTau internalization in astrocytes. Astrocyte functions are primarily regulated by intracellular Ca^{2+} transients (Scemes and Giaume, 2006). In primary cultures of astrocytes treated with either vehicle or ex-oTau we studied Ca^{2+} signals by confocal Ca^{2+} imaging. We started analyzing intracellular Ca^{2+} transients elicited by extracellular application of ATP and found that vehicle-treated astrocytes responded to ATP (100 μM for 10 s) with Ca^{2+} transients whose mean amplitude,

quantified as ΔF/F, was 14.3±1.2 (*n*=89; Fig. 2A). Moreover, ATP stimulation triggered spontaneous Ca^{2+} transients whose mean frequency and amplitude were: 22.5±0.7 oscillations/10 min and 1.9±0.3 ΔF/F, respectively (Fig. 2B). Cultured astrocytes treated for 1 hour with 100 nM ex-oTau exhibited a significant reduction in the amplitude of ATP-induced Ca^{2+} transients (8.0±0.7, *n*=92, P=1.1×10^{-5} assessed by two-tailed *t*-test [t=4.5, dof: 179]; Fig. 2A,C) as well as in the frequency (15.7±0.9 oscillations/10 min, P=4.2×10^{-8}) and amplitude (1.1±0.2 ΔF/F; P=0.004, t=5.7, dof: 179) of Ca^{2+} waves (Fig. 2B,D,E).

Tau treatment affects gliotransmitter release from astrocytes

It is known that ATP-induced calcium waves in astrocytes regulate the release of gliotransmitters, including glutamate, D-serine and ATP itself. ATP-induced ATP release contributes to sustain and propagate Ca^{2+} waves and the released ATP may be converted to ADP by ectonucleotidases in the extracellular medium (Burnstock, 2007). The ATP-dependent gliotransmitter release is directly involved in modulating synaptic transmission and plasticity (Zorec et al., 2016a; De Pittà et al., 2016). By using HPLC we measured the amount of gliotransmitters released extracellularly by cultured astrocytes during 1-hour treatment with either vehicle or 100 nM ex-oTau. To avoid any possible confounding effects exerted by components of the astrocyte culture medium, vehicle and tau treatments were carried out in Tyrode's solution, and gliotransmitters were measured in the conditioned medium (see methods). In agreement with the observed reduction in intracellular Ca^{2+} signals, we found that tau treatment significantly reduced the levels of gliotransmitters released extracellularly, with ATP being the most affected one. In fact, ATP levels were reduced by 73±7% respect to vehicle-treated cultures (from 93±27 to 28±13 nM; P=0.0053 assessed by Mann-Whitney test, *n*=5 replicates), whereas glutamate, glutamine and serine (both L- and D-) were reduced by 52±5% (from 0.91±0.14 to 0.45±0.11 μM), 61±14% (from 33.6±8.4 to 12.2±4.5 μM) and 55±2% (from 15.2±0.8 to 6.2±0.5 μM), respectively (P=0.036 for each comparison). Conversely, ADP levels increased following tau treatment (+28±13%; P=0.036; Fig. 3).

Tau-induced inhibition of synaptic vesicle release and synaptic protein expression are rescued by extracellular application of ATP

Previous works demonstrated that extracellular application of oTau affects synaptic function (Guerrero-Muñoz et al., 2015; Fà et al., 2016). It is also known that alterations in gliotransmitter release from astrocytes markedly influences synaptic transmission and plasticity. To determine the role of altered gliotransmitter release in tau-induced synaptic dysfunction, we performed patch-clamp and FM1-43 imaging experiments evaluating the impact of 1-hour ex-oTau treatment on basal synaptic transmission and synaptic vesicle release in mouse hippocampal neurons at DIV 14 grown in co-culture with astrocytes. We found that both the frequency and the amplitude of mEPSCs dropped from 5.9±0.6 Hz and 12.8±1.6 pA in vehicle-treated cells [*n*=27] to 3.2±0.5 Hz and 7.2±0.8 pA in cultures exposed to 100 nM ex-oTau for 1 hour [*n*=23] (two tailed Student's *t* test: P=1.1×10^{-3}; t=3.46; dof=48, and P=0.4×10^{-2}; t=-3.02; dof=48, respectively, Fig. 4A,B). The effects of oTau on basal synaptic transmission were dose-dependent. Indeed, the frequency and amplitude of mEPSCs after 1-h treatment with 10 nM oTau were 6.3±0.5 Hz and 10.6±1.1 pA, respectively [*n*=27], whereas these values were reduced to 3.1±0.4 Hz and 6.3±0.6 pA

[n=19] after application of higher doses of ex-oTau (1000 nM; Supplementary Fig. 2). One-way ANOVA performed among vehicle, 10, 100 and 1000 nM oTau ($F_{3,92}$=10.88 [P=3.0×10^{-6}] and $F_{3,92}$=6.62 [P=4.2×10^{-4}], respectively for frequency and amplitude) followed by SNK *post-hoc* test revealed that the differences between vehicle and 10 nM oTau were not statistically significant (P=0.556 for frequency and P=0.153 for amplitude of mEPSCs), whereas a significant difference was observed between 10 and 100 nM ex-oTau (P=5.1×10^{-4} and P=0.039 for frequency and amplitude, respectively). The effects of 1000 nM ex-oTau were instead similar to those of 100 nM (P=0.927 for frequency and P=0.619 for amplitude of mEPSCs), thus indicating that the latter concentration is sufficient to exert maximal impairment of synaptic transmission.

KCl-stimulated vesicular release (studied by FM1-43 imaging) was also significantly impaired in hippocampal neurons treated with 100 nM ex-oTau for 1 hour (P=0.032, Mann-Whitney test; n=10 and 7 for vehicle and tau, respectively; Fig. 4C). Synaptic function alterations following tau treatment were paralleled by a significant decrease in the expression of the presynaptic proteins synapsin-1 and synaptophysin, two key synaptic proteins involved in the release and fusion of neurotransmitter-containing synaptic vesicles, and the postsynaptic protein GluR1 which, as revealed by Western blot analysis, were reduced by 59±7%, 45±7% and 27±1% respectively (P=0.037 *vs.* vehicle assessed by Mann-Whitney test, n=3 replicates; Fig. 4D,E). These findings were also supported by consistent results obtained by immunocytochemistry (-48±6% vs. vehicle for synapsin-1 immunoreactivity [P=2.7×10^{-8} assessed by two-tailed Student's *t* test, t=8.07, dof=24]; -59±11% for synaptophysin; and -26±5% for GluR1 [P=5.1×10^{-5}; t=4.46, dof=47]; Fig. 4F-H). No significant modifications were instead found in the expression of PSD-95 or in the density of dendritic spines (Supplementary Fig. 3).

To better support our findings in the context of human AD pathology, in a subset of experiments we evaluated the effects of human AD Tau (i.e., derived from the brain of AD patients) on synaptic transmission, vesicular release and synaptic protein expression. We found that the inhibitory effects of 100 nM ex-AD Tau on mEPSCs was not significantly different from that of 100 nM recombinant tau (frequency: 3.5±0.3 *vs.* 6.7±0.4 Hz in controls [P=4.3×10^{-6} vehicle *vs.* AD Tau, t=5.35, dof=38; P=0.608 AD tau *vs.* oTau, t=-0.51, dof=43]; amplitude: 5.3±0.7 vs. 12.3±1.8 pA [P=2.6×10^{-4} vehicle *vs.* AD Tau, t=-4.02, dof=38; P=0.06 AD Tau *vs.* oTau, t=1.94, dof=43]). Similar results were also obtained for synaptic vesicle release and synaptic proteins expression (Supplementary Fig. 4).

Among the gliotransmitters released from astrocytes, ATP was the most affected by ex-oTau treatment. Notably, a reduction in extracellular ATP results in impaired intracellular Ca^{2+} signaling in astrocytes with the consequent reduction in the release of other gliotransmitters, especially glutamate and D-serine. Therefore, we checked whether the observed synaptotoxic effects of tau were reverted by restoring the extracellular levels of ATP. To address this issue, we repeated patch-clamp, FM1-43, Western blot and immunocytochemistry experiments in mixed cultures of hippocampal neurons and astrocytes treated for 1 hour with ex-oTau plus ATP. The presence of exogenous ATP (10 μM) in the culture medium during ex-oTau treatment completely spared neurons from the synaptotoxic effects of tau (Fig. 4A-H). In fact, one-way ANOVA test performed among vehicle, ex-oTau

and ex-oTau+ATP ($F_{2,71}$=5.90 [P=4.2×10^{-3}] and 5.48 [P=6.3×10^{-3}] for mEPSC frequency and amplitude, respectively) revealed no significant difference between vehicle and ex-oTau +ATP (*n*=24; P=0.34 and 0.79, for mEPSC frequency and amplitude, respectively; assessed by SNK *post-hoc* test). Instead, the difference between ex-oTau and ex-oTau+ATP was statistically significant for both parameters (P=0.02 for the frequency and 0.01 for the amplitude of mEPSCs; SNK test). Remarkably, ATP also reverted the detrimental effects of AD Tau on synaptic transmission (AD Tau *vs.* AD Tau+ATP, P=1.2×10^{-4} and 2.8×10^{-3} for frequency and amplitude of mEPSCs, SNK test). Similar results were also obtained for vesicular release evaluated by FM1-43 imaging (Fig. 4C), and protein expression evaluated through western blotting and immunocytochemistry (Fig. 4D-H) when cultures were treated with recombinant human oTau and ATP.

Collectively, these data suggest that the earliest synaptotoxic effects of tau rely on astrocyte dysfunction consisting of altered Ca^{2+}- and ATP-dependent release of gliotransmitters that, in turn, influences synaptic protein levels, synaptic vesicle release and post-synaptic currents in neighboring neurons. To further test this hypothesis, we mimicked the action of tau on astrocytes by metabolically inhibiting them with fluorocitrate (FC) (Swanson and Graham, 1994). Notably, fluorocitrate inhibits astrocytes without directly affecting neurons. We found that application of FC (100 μM) for 1.5 hours altered basal synaptic transmission and synaptic protein expression similarly to ex-oTau (Supplementary Fig. 5). In fact, ANOVA test revealed significant differences between vehicle- and FC-treated neurons in terms of frequency (3.1±0.4 Hz [*n*=25], $F_{2,67}$=9.91 [P=1.7×10^{-4}]; P=4.5×10^{-4} assessed by SNK *post-hoc* test) and amplitude (9.2±1.2 pA, respectively; $F_{2,67}$=4.56 [P=0.014]: P=0.026 assessed by SNK test) of mEPSCs but not between FC and ex-oTau (P=0.75 and P=0.51, respectively for frequency and amplitude, assessed by SNK test). Synaptic protein levels (e.g. synaptophysin) were also significantly lowered in FC-treated neurons with respect to vehicle-treated cultures.

APP is necessary for tau internalization in astrocytes and changes in intracellular Ca^{2+} signaling and gliotransmitter release

To validate the role of astrocytes in the synaptotoxic action of tau we investigated the effects of ex-oTau in hippocampal neurons plated onto astrocytes that are unable to upload tau from the extracellular medium. Previous studies demonstrated that internalization of extracellular tau depended on its interaction and binding with heparan sulfate proteoglycans (HSPG) (Holmes et al., 2013; Mirbaha et al., 2015). It is also known that APP and HSPG likely interact at the plasma membrane (Reinhard et al., 2013) and in the absence of proteins belonging to the APP superfamily HSPG are rapidly degraded (Cappai et al., 2005). Moreover, in 2015 Takahashi and colleagues demonstrated that the extracellular domain of APP is necessary for seed-dependent tau aggregation at extracellular level and accelerates intracellular tau aggregation, thus supporting the hypothesis that APP may act as a receptor for extracellular tau. Based on these observations we checked whether cells lacking APP were unable to upload ex-oTau. This hypothesis was verified by applying ex-oTau to co-cultures of astrocytes obtained from both APP-KO mice and WT mice expressing eGFP. Expression of eGFP in WT mice allowed us to distinguish the two cell populations. Consistent with our hypothesis, when IRIS-5-labelled oTau was applied to these co-cultures,

ex-oTau internalization was observed in WT but not in APP-KO astrocytes (Fig. 5A). Internalization index evaluated for APP-KO astrocytes was significantly lower respect to APP WT astrocytes (1.7±0.2 *vs.* 12.6±1.9, respectively; $P=1.5\times10^{-3}$; t=3.73, dof=18).

Next, we measured whether APP-KO astrocytes displayed changes in intracellular Ca^{2+} transients and waves following tau exposure. Treatment of APP-KO astrocyte cultures with 100 nM ex-oTau for 1 hour revealed no significant changes in the amplitude of ATP-induced Ca^{2+} transients with respect to vehicle-treated APP-KO astrocytes (9.6±0.5 *vs.* 10.0±0.8; n=42 and 45, respectively; Fig. 5B) although, as previously reported (Linde et al., 2011), the mean amplitude of Ca^{2+} transients was smaller than that of vehicle-treated WT astrocytes because of reduced Ca^{2+} levels in the endoplasmic reticulum. Similar results were obtained for Ca^{2+} wave frequency (21.4±1.6 *vs.* 20.9±2.1 oscillations/10 min, respectively) and amplitude (1.1±0.2 *vs.* 1.2±0.2; Fig. 5C,D) that were not affected by ex-oTau treatment. These data indicate that tau-induced alterations in intracellular Ca^{2+} signaling depend on tau internalization within astrocytes, and gliotransmitter release from APP-KO astrocytes was not affected by ex-oTau application (Fig. 5E).

Synaptic function is spared by tau-induced changes in WT neurons cultured on APP-KO astrocytes

To further investigate correlation among ex-oTau accumulation in astrocytes, altered gliotransmitter release and tau-induced synaptic changes, we cultured hippocampal neurons obtained from WT mice on a layer of astrocytes derived from APP-KO mice and exposed these co-cultures to 100 nM ex-oTau for 1 hour before studying basal synaptic transmission, KCl-mediated vesicular release, and the expression of synaptic proteins. In contrast to what occurred in WT neurons co-cultured with WT astrocytes, tau did not exert any significant adverse effects in WT neurons co-cultured with APP-KO astrocytes (Fig. 6A-G). Collectively, these findings support our hypothesis that altered gliotransmission following tau internalization in astrocytes underlies the earliest synaptotoxic action of tau.

Discussion

In this study, we demonstrated that extracellular application of both recombinant oligomeric tau and tau isolated from brains of AD patients depresses synaptic transmission *in vitro* through a mechanism directly involving the impairment of gliotransmitter release from astrocytes. Both astrocytes and neurons are targets of extracellular tau oligomers but, at least in the very early phases of tau exposure, astrocytes uploaded tau more rapidly and abundantly than neurons. After 1-hour exposure the accumulation of tau in neurons was very scarce and it became evident only after several hours of treatment (Fà et al., 2016). Therefore we used this experimental model (i.e., short-lasting tau treatments) to identify the specific contribution of astrocytes to the tau-induced synaptic dysfunction. Following 1-hour exposure to ex-oTau hippocampal neurons co-cultured with astrocytes exhibited: i) reduced levels of presynaptic and post-synaptic proteins (synapsin-1, synaptophysin and GluR1); ii) a significant decrease of evoked vesicular release; and iii) a significant reduction of mEPSC frequency and amplitude. These findings suggest that tau-accumulating astrocytes significantly contribute to the synaptic depression induced by oTau.

It is known that astrocytes strongly affect synaptic transmission through Ca^{2+}-dependent release of a plethora of gliotransmitters that include glutamate, D-serine and ATP (Araque et al., 1998; Fields and Burnstock, 2006; Jourdain et al., 2007; Perea and Araque, 2010; Zorec et al., 2016a). Calcium-dependent release of gliotransmitters have been reported to modulate synaptic transmission in a very complex way, depending on the type of gliotransmitter involved, the type of receptors it stimulates, and the pre- or postsynaptic localization of the receptor (De Pittà et al., 2016). For example, Ca^{2+}-dependent releases of glutamate and its co-agonist D-serine from astrocytes (that depend on extracellular ATP) may activate presynaptic NMDA receptors and/or metabotropic receptors as mGluR5 (D'Ascenzo et al., 2007; Fellin et al., 2007; Hamilton et al., 2010), as well as non-synaptic NMDARs (Araque et al., 1998), that increase the probability of neurotransmitter release. The same molecules may bind to receptors on the post-synaptic side thus also affecting the amplitude of excitatory post-synaptic currents. Consisting with these observations, we found that 1-hour treatment with ex-oTau causes alteration of evoked and spontaneous intracellular Ca^{2+} signaling that is fundamental for gliotransmitter release from astrocytes. Indeed, the amount of ATP, glutamate, serines, and glutamine released extracellularly by tau-treated astrocytes was significantly lowered if compared to vehicle-treated ones. On the contrary, ADP, that is obtained from extracellular ATP by the action of ectonucleotidases (Burnstock, 2007), increased significantly. We then cannot exclude that the higher reduction in ATP levels we observed following tau treatment, compared to the other gliotransmitters, may be partly due to degradation of extracellularly released ATP to ADP.

We have found tau-induced changes in synaptic function following ATP stimulation. The role of ATP in modulating synaptic transmission between neurons is quite controversial. ATP and its derivative purines, ADP and adenosine, are known to regulate synaptic transmission through the activation of a wide family of purinergic P2 receptors (ionotropic P2XRs and metabotropic P2YRs and their subfamily) located on the pre- and postsynaptic membranes thus resulting in a very complex modulation of glial-neuron crosstalk and synaptic transmission (Del Puerto et al., 2013; Fields and Burnstock, 2006; Lalo et al., 2016). If ATP released in the synaptic cleft binds ionotropic P2X receptors (e.g. 1, 2/3, and 3) at the presynaptic membrane it promotes glutamate release; on the contrary, if it binds metabotropic P2Y receptors (e.g. 1, 2 and/or 4) it triggers an inhibitory action (Koizumi et al., 2003; Pougnet et al., 2014; Rodrigues et al., 2005; Sun et al., 2016). Moreover, ATP itself, by activating metabotropic purinergic receptors P2Y located on the membrane of astrocytes, triggers intracellular IP_3 production that sustains intracellular Ca^{2+} waves and the consequent release of glutamate and D-serine (De Pittà et al., 2016). Finally, ADP and adenosine have been proven to have an inhibitory effect on glutamatergic transmission (Pascual et al., 2005).

Do the inhibitory effects we observed in hippocampal neurons after ex-oTau exposure depend on the reduced expression of synaptic proteins following impaired gliotransmitter release, or on a direct effect of the gliotransmitters? Our functional measurements (i.e., patch-clamp recordings and FM1-43 imaging) were carried out in Tyrode's solution that did not contain either ATP or other gliotransmitters. Therefore, the inhibition of synaptic transmission we observed after tau treatment is unlikely to depend upon a “direct” receptor activation by gliotransmitters. It is likely, instead, that the reduced release of ATP, glutamate

and D-serine from tau-accumulating astrocytes, along with the increased ADP levels, have a net negative impact on the molecular machinery controlling synaptic transmission through changes in synaptic protein expression.

The ability of ex-oTau to reduce presynaptic protein expression in mice was proposed some years ago (Lasagna-Reeves et al., 2011) and a few papers have reported that tau-transgenic mice exhibiting accumulation of oTau also display a significant reduction of synatophysin (Garringer et al., 2013; Yoshiyama et al., 2007). We have now demonstrated that administration of extracellular ATP to the culture medium of tau-treated neurons prevents the synaptotoxic action of tau, thus indicating that the effects of tau on synaptic protein expression and synaptic transmission involve extracellular ATP availability. These results are in line with those of Jung and co-workers (Jung et al., 2012) that demonstrated the protective action of extracellular ATP against $A\beta_{42}$ synaptotoxic action.

Further confirmation that astrocytes mediate the early synaptotoxic action of tau by reducing the availability of ATP, and ATP-dependent gliotransmitters in the extracellular space, comes from experiments carried out after metabolically inhibiting astrocytes with fluorocitrate (that targets astrocytes but not neurons) and from experiments in which WT hippocampal neurons were plated on a monolayer of APP-KO astrocytes. In the former experiments hippocampal neurons co-cultured with FC-inhibited astrocytes exhibited the same synaptic alterations of tau-treated cultures; in the latter, hippocampal neurons bearing APP (that may internalize ex-oTau) co-cultured with APP-KO astrocytes (that cannot internalize ex-oTau and are not affected by tau treatment in terms of Ca^{2+}-dependent gliotransmitter release) did not exhibit alterations in miniature release of neurotransmitter, synaptic vesicle release, and synaptic protein expression following 1-hour tau treatment.

Remarkably, results of our immunocytochemical experiments provide novel evidence that APP expression is fundamental for tau uploading from astrocytes. Different mechanisms may underlie APP-mediated tau internalization: i) APP may act as receptor for tau, as proposed for uptake of extracellular fibrils (Takahashi et al., 2015); or ii) it may affect HPSG expression (Cappai et al., 2005; Reinhard et al., 2013) that has been also demonstrated to be necessary for tau internalization in neurons (Holmes et al., 2013; Mirbaha et al., 2015).

In conclusion, our data demonstrate that astrocytes significantly contribute to the synaptotoxic action of oTau likely cooperating with the direct action exerted by this misfolded protein in neurons (Fà et al., 2016). Tau rapidly and abundantly internalizes in astrocytes, alters spontaneous intracellular Ca^{2+} transients in these cells thus reducing the amount of ATP and the other gliotransmitters released in the extracellular medium. The reduced availability of gliotransmitters, along with the increased levels of inhibitory purines, such as ADP, negatively impacts on presynaptic vesicular release thus leading to a reduction of synaptic protein expression and a depressed transmission in the neighboring neurons. *In vivo*, the scenario is more complex than that analyzed in our experimental models because of brain mechanisms other than purinergic signals (e.g. adrenergic signals) modulating glial function and glial-to-neuron communication in response to stressful and/or pathological stimuli (Braun et al., 2014; Franke et al., 2012). Nonetheless, our findings unveil the critical role played by altered gliotransmission in the tau-induced synaptic deficits thus contributing

to advance our understanding of the cellular and molecular mechanisms underlying progressive cognitive decline and memory loss in tauopathies, including AD, caused by accumulation of misfolded tau protein in the brain.

Supplementary Material

Refer to Web version on PubMed Central for supplementary material.

Acknowledgments

This work was supported by Università Cattolica Intramural Funds to CG and NIH grant R01AG049402 to OA. We wish to thank Dr. Mauro Fà for advice on recombinant tau preparation and tau purification from patients, and Dr. Agnieszka Staniszewski for help with tau preparation. The authors declare no conflicts of interest.

References

Amorini AM, Giorlandino C, Longo S, D'Urso S, Mesoraca A, Santoro ML, Picardi M, Gullotta S, Cignini P, Lazzarino D, Lazzarino G, Tavazzi B. Metabolic profile of amniotic fluid as a biochemical tool to screen for inborn errors of metabolism and fetal anomalies. Mol Cell Biochem. 2012; 359:205–216. [PubMed: 21837404]

Amorini AM, Lazzarino G, Di Pietro V, Signoretti S, Lazzarino G, Belli A, Tavazzi B. Severity of experimental traumatic brain injury modulates changes in concentration of cerebral free amino acids. J Cell Mol Med. 2016; In press. doi: 10.11/jcmm.12998

Araque A, Sanzgiri RP, Parpura V, Haydon PG. Calcium elevation in astrocytes causes an NMDA receptor-dependent increase in the frequency of miniature synaptic currents in cultured hippocampal neurons. J Neurosci. 1998; 18:6822–6829. [PubMed: 9712653]

Asai H, Ikezu S, Tsunoda S, Medalla M, Luebke J, Haydar T, Wolozin B, Butovsky O, Kügler S, Ikezu T. Depletion of microglia and inhibition of exosome synthesis halt tau propagation. Nat neurosci. 2015; 18:1584–1593. [PubMed: 26436904]

Bolós M, Llorens-Martín M, Jurado-Arjona J, Hernández F, Rábano A, Avila J. Direct Evidence of Internalization of Tau by Microglia In Vitro and In Vivo. J Alzheimers Dis. 2016; 50:77–87. [PubMed: 26638867]

Bosch M, Castro J, Saneyoshi T, Matsuno H, Sur M, Hayashi Y. Structural and molecular remodeling of dendritic spine substructures during long-term potentiation. Neuron. 2014; 82:444–459. [PubMed: 24742465]

Braun D, Madrigal JL, Feinstein DL. Noradrenergic regulation of glial activation: molecular mechanisms and therapeutic implications. Curr Neuropharmacol. 2014; 12:342–352. [PubMed: 25342942]

Burnstock G. Physiology and pathophysiology of purinergic neurotransmission. Physiol Rev. 2007; 87:659–797. [PubMed: 17429044]

Cappai R, Cheng F, Ciccotosto GD, Needham BE, Masters CL, Multhaup G, Fransson LA, Mani K. The amyloid precursor protein (APP) of Alzheimer disease and its paralog, APLP2, modulate the Cu/Zn-Nitric Oxide-catalyzed degradation of glypican-1 heparan sulfate in vivo. J Biol Chem. 2005; 280:13913–13920. [PubMed: 15677459]

D'Ascenzo M, Fellin T, Terunuma M, Revilla-Sanchez R, Meaney DF, Auberson YP, Moss SJ, Haydon PG. mGluR5 stimulates gliotransmission in the nucleus accumbens. Proc Natl Acad Sci USA. 2007; 104:1995–2000. [PubMed: 17259307]

De Pittà M, Brunel N, Volterra A. Astrocytes: Orchestrating synaptic plasticity? Neuroscience. 2016; 323:43–61. [PubMed: 25862587]

Del Puerto A, Wandosell F, Garrido JJ. Neuronal and glial purinergic receptors functions in neuron development and brain disease. Front Cell Neurosci. 2013; 7:197. [PubMed: 24191147]

Díaz-Hernández M, Gómez-Ramos A, Rubio A, Gómez-Villafuertes R, Naranjo JR, Miras-Portugal MT, Avila J. Tissue-nonspecific alkaline phosphatase promotes the neurotoxicity effect of extracellular tau. J Biol Chem. 2010; 285:32539–32548. [PubMed: 20634292]

Fá M, Puzzo D, Piacentini R, Staniszewski A, Zhang H, Baltrons MA, Li Puma DD, Chatterjee I, Li J, Saeed F, Berman HL, Ripoli C, Gulisano W, Gonzalez J, Tian H, Costa JA, Lopez P, Davidowitz E, Yu WH, Haroutunian V, Brown LM, Palmeri A, Sigurdsson EM, Duff KE, Teich AF, Honig LS, Sierks M, Moe JG, D'Adamio L, Grassi C, Kanaan NM, Fraser PE, Arancio O. Extracellular Tau Oligomers Produce An Immediate Impairment of LTP and Memory. Sci Rep. 2016; 6:19393. [PubMed: 26786552]

Fellin T, D'Ascenzo M, Haydon PG. Astrocytes control neuronal excitability in the nucleus accumbens. ScientificWorldJournal. 2007; 7:89–97. [PubMed: 17982581]

Fields RD, Burnstock G. Purinergic signalling in neuron-glia interactions. Nat Rev Neurosci. 2006; 7:423–436. [PubMed: 16715052]

Forman MS, Lal D, Zhang B, Dabir DV, Swanson E, Lee VM, Trojanowski JQ. Transgenic mouse model of tau pathology in astrocytes leading to nervous system degeneration. J Neurosci. 2005; 25:3539–3550. [PubMed: 15814784]

Franke H, Verkhratsky A, Burnstock G, Illes P. Pathophysiology of astroglial purinergic signalling. Purinergic Signal. 2014; 8:629–657.

Gaffield MA, Betz WJ. Imaging synaptic vesicle exocytosis and endocytosis with FM dyes. Nat Protoc. 2006; 1:2916–2921. [PubMed: 17406552]

Gao V, Suzuki A, Magistretti PJ, Lengacher S, Pollonini G, Steinman MQ, Alberini CM. Astrocytic β2-adrenergic receptors mediate hippocampal long-term memory consolidation. Proc Natl Acad Sci USA. 2016; 113:8526–8531. [PubMed: 27402767]

Garringer HJ, Murrell J, Sammeta N, Gnezda A, Ghetti B, Vidal R. Increased tau phosphorylation and tau truncation, and decreased synaptophysin levels in mutant BRI2/tau transgenic mice. PLoS One. 2013; 8:e56426. [PubMed: 23418567]

Giaume C, Oliet S. Introduction to the special issue: Dynamic and metabolic interactions between astrocytes and neurons. Neuroscience. 2016; 323:1–2. [PubMed: 26940478]

Guerrero-Muñoz MJ, Gerson J, Castillo-Carranza DL. Tau Oligomers: The Toxic Player at Synapses in Alzheimer's Disease. Front Cell Neurosci. 2015; 9:464. [PubMed: 26696824]

Hamilton NB, Attwell D. Do astrocytes really exocytose neurotransmitters? Nat Rev Neurosci. 2010; 11:227–238. [PubMed: 20300101]

Holmes BB, DeVos SL, Kfoury N, Li M, Jacks R, Yanamandra K, Ouidja MO, Brodsky FM, Marasa J, Bagchi DP, Kotzbauer PT, Miller TM, Papy-Garcia D, Diamond MI. Heparan sulfate proteoglycans mediate internalization and propagation of specific proteopathic seeds. Proc Natl Acad Sci USA. 2013; 110:E3138–E3147. [PubMed: 23898162]

Iacopino F, Angelucci C, Piacentini R, Biamonte F, Mangiola A, Maira G, Grassi C, Sica G. Isolation of cancer stem cells from three human glioblastoma cell lines: characterization of two selected clones. PLoS One. 2014; 9:e105166. [PubMed: 25121761]

Jourdain P, Bergersen LH, Bhaukaurally K, Bezzi P, Santello M, Domercq M, Matute C, Tonello F, Gundersen V, Volterra A. Glutamate exocytosis from astrocytes controls synaptic strength. Nat Neurosci. 2007; 10:331–339. [PubMed: 17310248]

Jung ES, An K, Hong HS, Kim JH, Mook-Jung I. Astrocyte-originated ATP protects Aβ(1-42)-induced impairment of synaptic plasticity. J Neurosci. 2012; 32:3081–3087. [PubMed: 22378880]

Kahlson MA, Colodner KJ. Glial Tau Pathology in Tauopathies: Functional Consequences. J Exp Neurosci. 2016; 9(Suppl 2):43–50. [PubMed: 26884683]

Kampers T, Pangalos M, Geerts H, Wiech H, Mandelkow E. Assembly of paired helical filaments from mouse tau: implications for the neurofibrillary pathology in transgenic mouse models for Alzheimer's disease. FEBS Lett. 1999; 451:39–44. [PubMed: 10356980]

Koizumi S, Fujishita K, Tsuda M, Shigemoto-Mogami Y, Inoue K. Dynamic inhibition of excitatory synaptic transmission by astrocyte-derived ATP in hippocampal cultures. Proc Natl Acad Sci USA. 2003; 100:11023–11028. [PubMed: 12958212]

Lalo U, Palygin O, Verkhratsky A, Grant SG, Pankratov Y. ATP from synaptic terminals and astrocytes regulates NMDA receptors and synaptic plasticity through PSD-95 multi-protein complex. Sci Rep. 2016; 6:33609. [PubMed: 27640997]

Lasagna-Reeves CA, Castillo-Carranza DL, Sengupta U, Clos AL, Jackson GR, Kayed R. Tau oligomers impair memory and induce synaptic and mitochondrial dysfunction in wild-type mice. Mol Neurodegener. 2011; 6:39. [PubMed: 21645391]

Lasagna-Reeves CA, Sengupta U, Castillo-Carranza D, Gerson JE, Guerrero-Munoz M, Troncoso JC, Jackson GR, Kayed R. The formation of tau pore-like structures is prevalent and cell specific: possible implications for the disease phenotypes. Acta Neuropathol Commun. 2014; 2:56. [PubMed: 24887264]

Linde CI, Baryshnikov SG, Mazzocco-Spezzia A, Golovina VA. Dysregulation of Ca^{2+} signaling in astrocytes from mice lacking amyloid precursor protein. Am J Physiol Cell Physiol. 2011; 300:C1502–1512. [PubMed: 21368296]

Luo W, Liu W, Hu X, Hanna M, Caravaca A, Paul SM. Microglial internalization and degradation of pathological tau is enhanced by an anti-tau monoclonal antibody. Sci Rep. 2015; 5:11161. [PubMed: 26057852]

Maiti P, Piacentini R, Ripoli C, Grassi C, Bitan G. Surprising toxicity and assembly behaviour of amyloid β-protein oxidized to sulfone. Biochem J. 2011; 433:323–32. [PubMed: 21044048]

Maphis N, Xu G, Kokiko-Cochran ON, Jiang S, Cardona A, Ransohoff RM, Lamb BT, Bhaskar K. Reactive microglia drive tau pathology and contribute to the spreading of pathological tau in the brain. Brain. 2015; 138:1738–1755. [PubMed: 25833819]

Medina M, Avila J. The role of extracellular Tau in the spreading of neurofibrillary pathology. Front Cell Neurosci. 2014; 8:113. [PubMed: 24795568]

Michel CH, Kumar S, Pinotsi D, Tunnacliffe A, St George-Hyslop P, Mandelkow E, Mandelkow EM, Kaminski CF, Kaminski Schierle GS. Extracellular monomeric tau protein is sufficient to initiate the spread of tau protein pathology. J Biol Chem. 2013; 289:956–67. [PubMed: 24235150]

Mirbaha H, Holmes BB, Sanders DW, Bieschke J, Diamond MI. Tau trimers are the minimal propagation unit spontaneously internalized to seed intracellular aggregation. J Biol Chem. 2015; 290:14893–14903. [PubMed: 25887395]

Pascual O, Casper KB, Kubera C, Zhang J, Revilla-Sanchez R, Sul JY, Takano H, Moss SJ, McCarthy K, Haydon PG. Astrocytic purinergic signaling coordinates synaptic networks. Science. 2005; 310:113–116. [PubMed: 16210541]

Perea G, Araque A. GLIA modulates synaptic transmission. Brain Res Rev. 2010; 63:93–102. [PubMed: 19896978]

Piacentini R, Li Puma DD, Ripoli C, Marcocci ME, De Chiara G, Garaci E, Palamara AT, Grassi C. Herpes Simplex Virus type-1 infection induces synaptic dysfunction in cultured cortical neurons via GSK-3 activation and intraneuronal amyloid-β protein accumulation. Sci Rep. 2015; 5:15444. [PubMed: 26487282]

Podda MV, Leone L, Piacentini R, Cocco S, Mezzogori D, D'Ascenzo M, Grassi C. Expression of olfactory-type cyclic nucleotide-gated channels in rat cortical astrocytes. Glia. 2012; 60:1391–1405. [PubMed: 22653779]

Pooler AM, Phillips EC, Lau DH, Noble W, Hanger DP. Physiological release of endogenous tau is stimulated by neuronal activity. EMBO Rep. 2013; 14:389–394. [PubMed: 23412472]

Pougnet JT, Toulme E, Martinez A, Choquet D, Hosy E, Boué-Grabot E. ATP P2X receptors downregulate AMPA receptor trafficking and postsynaptic efficacy in hippocampal neurons. Neuron. 2014; 83:417–430. [PubMed: 25033184]

Reinhard C, Borgers M, David G, De Strooper B. Soluble amyloid-β precursor protein binds its cell surface receptor in a cooperative fashion with glypican and syndecan proteoglycans. J Cell Sci. 2013; 126:4856–4861. [PubMed: 23986479]

Ripoli C, Piacentini R, Riccardi E, Leone L, Li Puma DD, Bitan G, Grassi C. Effects of different amyloid β-protein analogues on synaptic function. Neurobiol Aging. 2013; 34:1032–1044. [PubMed: 23046860]

Ripoli C, Cocco S, Li Puma DD, Piacentini R, Mastrodonato A, Scala F, Puzzo D, D'Ascenzo M, Grassi C. Intracellular accumulation of amyloid-β (Aβ) protein plays a major role in Aβ-induced

alterations of glutamatergic synaptic transmission and plasticity. J Neurosci. 2014; 34:12893–12903. [PubMed: 25232124]

Rodrigues RJ, Almeida T, Richardson PJ, Oliveira CR, Cunha RA. Dual presynaptic control by ATP of glutamate release via facilitatory P2X1, P2X2/3, and P2X3 and inhibitory P2Y1, P2Y2, and/or P2Y4 receptors in the rat hippocampus. J Neurosci. 2005; 25:6286–6295. [PubMed: 16000618]

Santoro M, Piacentini R, Masciullo M, Bianchi ML, Modoni A, Podda MV, Ricci E, Silvestri G, Grassi C. Alternative splicing alterations of Ca^{2+} handling genes are associated with Ca^{2+} signal dysregulation in myotonic dystrophy type 1 (DM1) and type 2 (DM2) myotubes. Neuropathol Appl Neurobiol. 2014; 40:464–476. [PubMed: 23888875]

Scemes E, Giaume C. Astrocyte calcium waves: what they are and what they do. Glia. 2006; 54:716–725. [PubMed: 17006900]

Sun XD, Li L, Liu F, Huang ZH, Bean JC, Jiao HF, Barik A, Kim SM, Wu H, Shen C, Tian Y, Lin TW, Bates R, Sathyamurthy A, Chen YJ, Yin DM, Xiong L, Lin HP, Hu JX, Li BM, Gao TM, Xiong WC, Mei L. Lrp4 in astrocytes modulates glutamatergic transmission. Nat Neurosci. 2016; 19:1010–1018. [PubMed: 27294513]

Swanson RA, Graham SH. Fluorocitrate and fluoroacetate effects on astrocyte metabolism in vitro. Brain Res. 1994; 664:94–100. [PubMed: 7895052]

Takahashi M, Miyata H, Kametani F, Nonaka T, Akiyama H, Hisanaga S, Hasegawa M. Extracellular association of APP and tau fibrils induces intracellular aggregate formation of tau. Acta Neuropathol. 2015; 129:895–907. [PubMed: 25869641]

Tavazzi B, Lazzarino G, Leone P, Amorini AM, Bellia F, Janson CG, Di Pietro V, Ceccarelli L, Donzelli S, Francis JS, Giardina B. Simultaneous high performance liquid chromatographic separation of purines, pyrimidines, N-acetylated amino acids, and dicarboxylic acids for the chemical diagnosis of inborn errors of metabolism. Clin Biochem. 2005; 38:997–1008. [PubMed: 16139832]

Togo T, Dickson DW. Tau accumulation in astrocytes in progressive supranuclear palsy is a degenerative rather than a reactive process. Acta Neuropathol. 2002; 104:398–402. [PubMed: 12200627]

Verkhratsky A, Zorec R, Rodriguez JJ, Parpura V. Pathobiology Of Neurodegeneration: The Role For Astroglia. Opera Med Physiol. 2016; 1:13–22. [PubMed: 27308639]

Yamada K, Holth JK, Liao F, Stewart FR, Mahan TE, Jiang H, Cirrito JR, Patel TK, Hochgräfe K, Mandelkow EM, Holtzman DM. Neuronal activity regulates extracellular tau in vivo. J Exp Med. 2014; 211:387–393. [PubMed: 24534188]

Yoshiyama Y, Higuchi M, Zhang B, Huang SM, Iwata N, Saido TC, Maeda J, Suhara T, Trojanowski JQ, Lee VM. Synapse loss and microglial activation precede tangles in a P301S tauopathy mouse model. Neuron. 2007; 53:337–351. [PubMed: 17270732]

Wu JW, Herman M, Liu L, Simoes S, Acker CM, Figueroa H, Steinberg JI, Margittai M, Kayed R, Zurzolo C, Di Paolo G, Duff KE. Small misfolded Tau species are internalized via bulk endocytosis and anterogradely and retrogradely transported in neurons. J Biol Chem. 2013; 288:1856–1870. [PubMed: 23188818]

Zorec R, Verkhratsky A, Rodríguez JJ, Parpura V. Astrocytic vesicles and gliotransmitters: Slowness of vesicular release and synaptobrevin2-laden vesicle nanoarchitecture. Neuroscience. 2016a; 323:67–75. [PubMed: 25727638]

Zorec R, Parpura V, Vardjan N, Verkhratsky A. Astrocytic face of Alzheimer's disease. Behav Brain Res. 2016b In press. doi:http://dx.doi.org/10.1016/j.bbr.2016.05.02.

Main Points

1. Tau oligomers enter astrocytes more efficiently than neurons.
2. Tau treatment affects Ca^{2+}-dependent gliotransmitter release.
3. Tau induces ATP-dependent inhibition of synaptic protein expression and synaptic transmission.

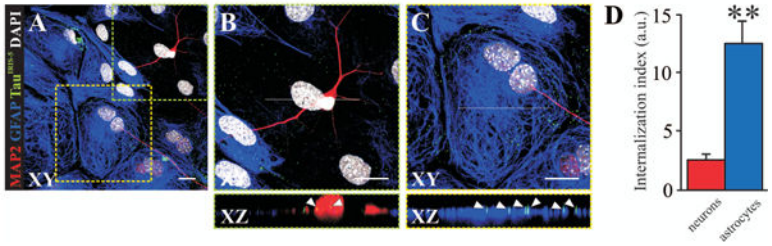

Figure 1. ex-oTau enters astrocytes more efficiently than neurons *in vitro*

(A) Representative example of tau accumulation in cultured hippocampal astrocytes and neurons. Tau (100 nM) was labelled with IRIS-5 ester dye at the N-terminus (here visualized in green to increase contrast) and then applied to the culture medium for 1 hour. Neurons were recognized by their immunoreactivity for the microtubule associated protein 2 (MAP2, visualized in red) and astrocytes were recognized by their immunoreactivity for Glial Fibrillary Acidic Protein (GFAP, visualized in blue). DAPI (shown in white) was used to identify cell nuclei. **(B, C)** Enlargements of dotted boxes outlined in (A) showing tau accumulation in a neuron (B) and an astrocyte (C). Bottom images represent XZ cross-sections from the Z-stack acquisitions showing internalization of tau in MAP2- and GFAP-positive cells (DAPI signal has been removed to allow tau quantification). Scale bars: 10 μm. **(D)** Bar graph showing the "internalization index" evaluated in neurons (MAP2) and astrocytes (GFAP) from the same cultures ** P<0.0001 *vs.* neurons.

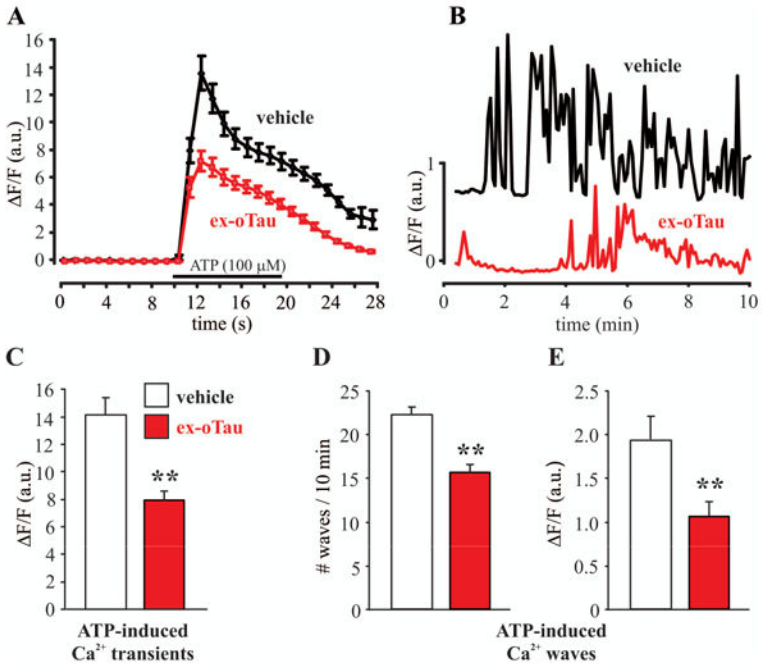

Figure 2. Ex-oTau treatment affects intracellular Ca^{2+} signals in cultured astrocytes

(A) Mean time-course of ATP-induced intracellular Ca^{2+} transients in Fluo-4-loaded mouse cultured astrocytes treated with either vehicle or ex-oTau (100 nM) for 1 hour. **(B)** Representative examples of ATP-elicited Ca^{2+} waves in astrocytes treated as in (A). **(C)** Bar graph showing the mean peak amplitude of ATP-induced Ca^{2+} transients. **(D,E)** Bar graphs showing the mean frequency and amplitude of Ca^{2+} waves in vehicle- and oTau-treated cultured astrocytes. ** P<0.001

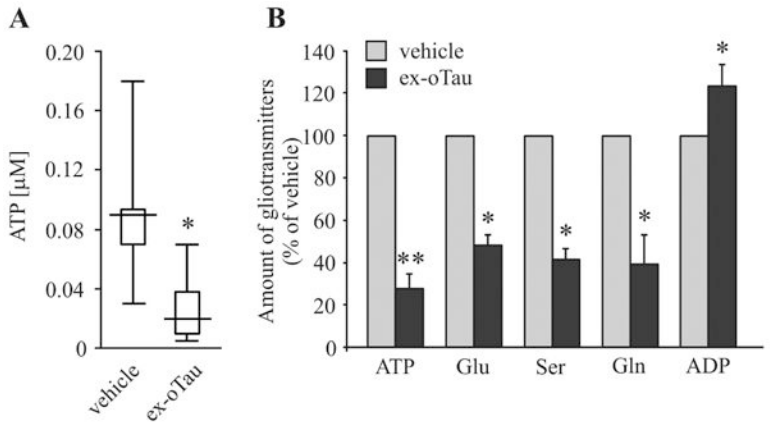

Figure 3. Ex-oTau treatment affects gliotransmitter release from cultured astrocytes

(A) Bar graphs quantifying the amount of ATP released extracellularly from cultured astrocytes during 1-hour treatment with either vehicle or ex-oTau (100 nM) and evaluated by HPLC. Data are presented as median with interquartile range; whiskers are the minimum and maximum. **(B)** Bar graphs summarizing the amount of various gliotransmitters released in the culture medium of astrocytes following 1-hour treatment with either vehicle or ex-oTau (100 nM). Values are normalized with respect to vehicle. * $P<0.05$ and ** $P<0.001$ *vs.* vehicle.

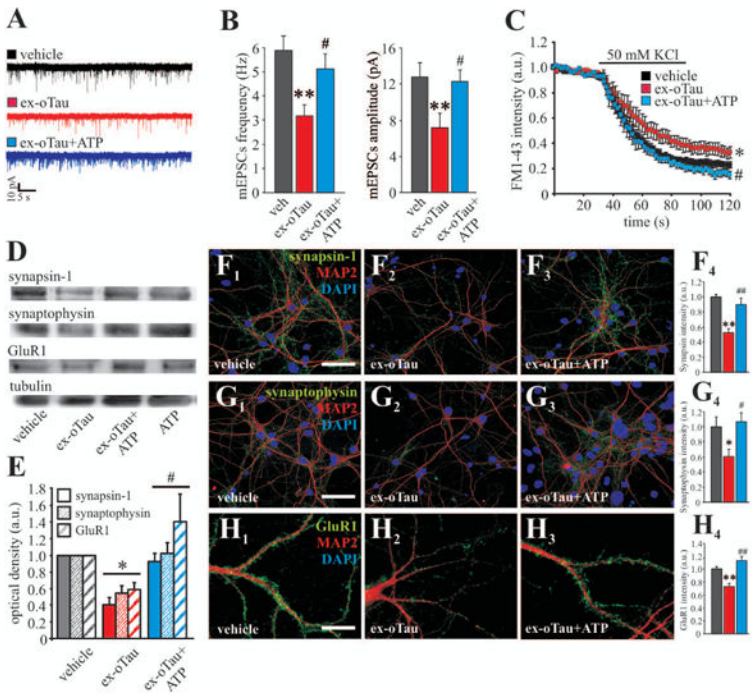

Figure 4. Exogenous ATP reverts the synaptic effects of ex-oTau

(A) Representative examples of miniature excitatory post-synaptic currents (mEPSCs) recorded from neurons treated with vehicle, 100 nM ex-oTau or ex-oTau+ATP (10 μM) for 1 hour. **(B)** Bar graphs showing the mean frequencies and amplitudes of mEPSCs recorded from neurons treated with vehicle [*n*=20], 100 nM ex-oTau [*n*=18], or ex-oTau+ATP (10 μM) [*n*=17] for 1 hour. **(C)** Mean time course of FM1-43 intensity following 50 mM KCl stimulation in neurons treated as in (A, B) [*n*=10 for vehicle and 7 for both ex-oTau and ex-oTau]. **(D)** Representative Western blot analysis of synapsin-1, synaptophysin and GluR1 performed on lysates of neuronal cultures treated for 1 hour with vehicle, 100 nM ex-oTau or ex-oTau+ATP (10 μM). Tubulin was used as loading control. **(E)** Densitometric analysis of three independent Western blot experiments carried out as in D. **(F-H)** Representative examples of confocal images of neuronal cultures treated with vehicle, 100 nM oTau or oTau +ATP (10 μM) for 1 hour and immunostained for the neuronal marker MAP2 and the presynaptic proteins synapsin-1 (F), synaptophysin (G), and the postsynaptic protein GluR1 (H). Bar graphs showing mean fluorescence intensity of synapsin-1 (F_4) synaptophysin (G_4) and GluR1 (H_4) in the panels $F_{1\text{-}3}$-$H_{1\text{-}3}$. Scale bar 20 μm. * P<0.05 *vs.* vehicle; ** P<0.005 *vs.* vehicle; # P<0.05 *vs.* tau,## P<0.005 *vs.* tau. Statistical significance was assessed by one-way ANOVA followed by Student-Newman-Keuls' test.

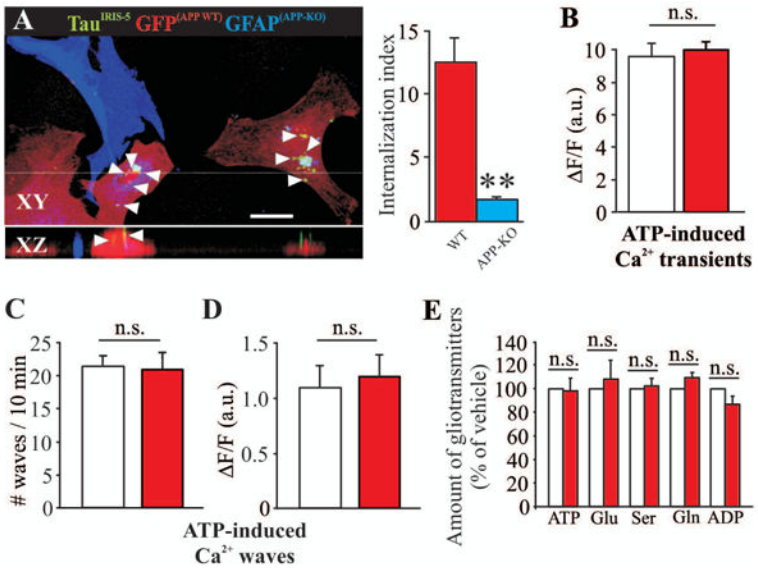

Figure 5. APP-KO astrocytes do not internalize tau and are unaffected by ex-oTau application

(A) Example of co-culture of APP-KO astrocytes (immunostained with anti-GFAP and visualized in blue) and WT-eGFP astrocytes (visualized in red) treated for 7 hours with IRIS-5-labelled tau (visualized in green). Arrowheads indicate tau spots that are present in WT-eGFP astrocytes only. Bottom image represents XZ cross-sections from the Z-stack acquisitions showing internalization of tau in GFP-positive astrocytes. Bar graph on the right shows the "internalization index" evaluated in APP-WT (red) and APP-KO (blue) astrocytes ** P<0.005 KO *vs.* WT. Scale bar: 10 μm. **(B)** Bar graph showing the mean peak amplitudes of ATP-induced Ca^{2+} transients. In this and the other panels white bars referred to vehicle whereas red ones referred to ex-oTau. **(C,D)** Bar graphs showing the mean frequency and amplitude of Ca^{2+} waves in vehicle- and ex-oTau-treated cultured APP-KO astrocytes. **(E)** Bar graphs indicating the amount of gliotransmitters released from astrocytes following 1-hour treatment with either vehicle or ex-oTau (100 nM) and measured by HPLC. Values are normalized with respect to vehicle. "n.s." means not statistically significant difference.

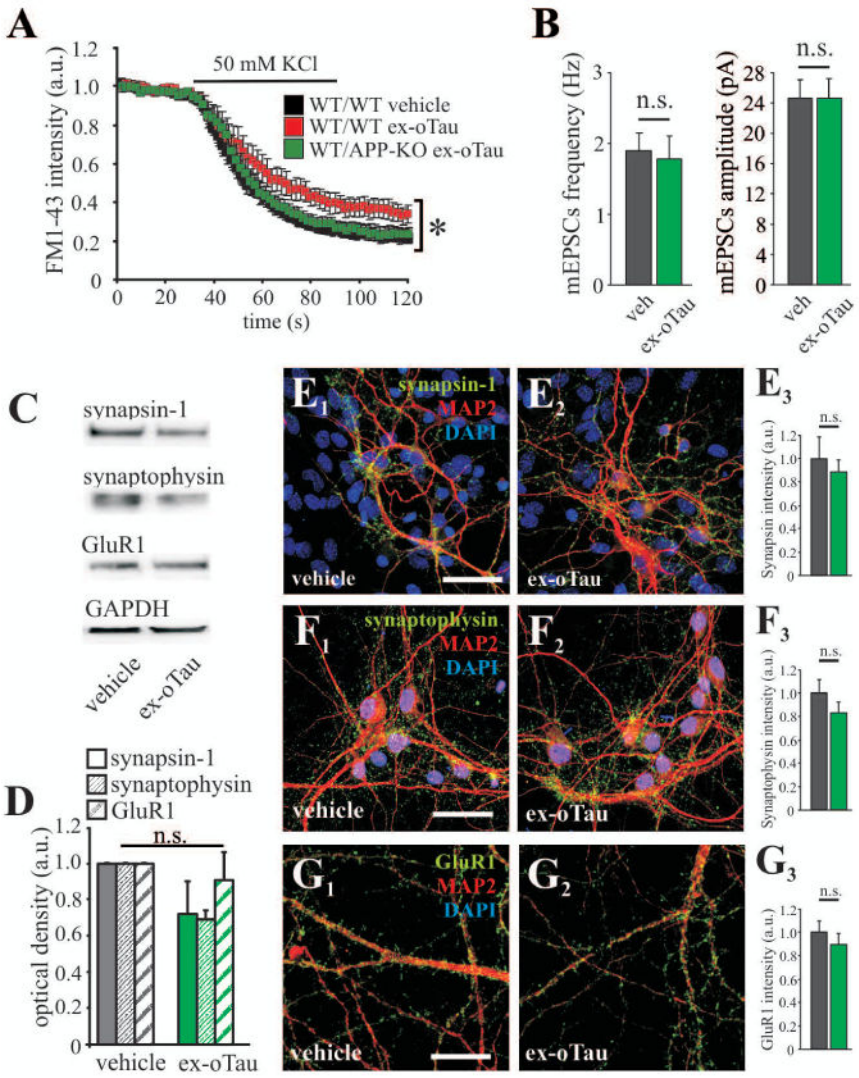

Figure 6. Synaptic function in WT hippocampal neurons plated on APP-KO astrocytes is not affected by ex-oTau

(A) Time course of FM1-43 intensity following 1-hour ex-oTau (100 nM) treatment of hippocampal WT neurons plated on a layer of either WT astrocytes (WT/WT tau; red trace) or APP-KO astrocytes (WT/APP-KO tau; green trace), compared with that of WT neurons plated on a layer of WT astrocytes exposed to vehicle (WT/WT vehicle). Vesicular release was induced by depolarizing neurons with 50 mM KCl. **(B)** Bar graphs showing the mean frequencies and amplitudes of mEPSCs recorded from WT neurons plated on APP-KO astrocytes and treated with either vehicle [n=14] or 100 nM ex-oTau [n=25] for 1 hour. **(C)** Representative Western blot analysis of synapsin-1, synaptophysin and GluR1 performed on lysates hippocampal WT neurons plated on a layer of APP-KO astrocytes and treated with either vehicle or 100 nM ex-oTau. GAPDH was used as loading control. (**D**) Densitometric analysis of three independent western blot experiments carried out as in C. (**E-G**) Representative examples of WT hippocampal neurons immunostained for the neuronal marker MAP2 and the synaptic proteins synapsin-1, synaptophysin and GluR1. Bar graphs

quantifying synapsin-1 (E_3), synaptophysin (F_3) and GluR1 (G_3) after treatment with vehicle or ex-oTau. Scale bars: 20 μm for panels E,F; 10 μm for panel G; *P<0.05.